Effects of Drive System Lubricant Additives upon Rolling Fatigue of Carburized and Hardened Steel Rollers

Akira YOSHIDA[*], Yuji OHUE[*] and Masahiro FUJII[*]

SYNOPSIS

To clarify the effects of a drive system lubricant additive upon rolling fatigue of rollers manufactured from carburized and hardened steel, three types of oil were used as lubricants: one mineral base oil and the other two mineral base oils to which an S-P additive package and ATF additive package were added, respectively. These specimens were tested for sliding/rolling fatigue and examined for failure on the surface, rolling fatigue strength, and other properties.

Roller surface temperatures and inter-roller frictional coefficients were found scarcely affected by the type of oil used. Irrespective of the difference in oil type, failure on the surface was found to be entirely spalling attributable to cracks generated in the subsurface. The depth at which spalling cracks had taken place was found nearly coincident with the depth at which a ratio of reversing orthogonal shear stress to hardness had amplitude $A(\tau_{yz}/Hv)$ maximized. These depths were larger as Hertz stress became more prominent. Nevertheless, they were found hardly affected by the type of oil. Although rolling fatigue strength did not show a significant difference dependent upon the type of oil, it may be said that fatigue life would be somewhat negatively affected by an extreme pressure coated film with a content of sulfur and phosphorus.

---

* Department of Mechanical Engineering

1. INTRODUCTION

Recently, a variety of oils are being developed as automotive gearing lubricants. Carburized/hardened steel applied to an MTX final reduction gear on a front-engine and front-driven vehicle has been bench-tested with a mounted helical gear. The results of this test show that compared lubricant to which nothing was added, a higher anti-pitting resistance was found available when an ATF additive package was applied to a mineral base oil of relatively low viscosity which contained a viscosity index improver, an anti-oxidant and a defoaming agent. To identify the effects of a drive system lubricant additive on rolling fatigue of carburized/hardened steel rollers, sliding/rolling fatigue tests were conducted using three oils. One oil was mineral-based and contained a viscosity index improver (of higher viscosity than that applied in the bench test), an anti-oxident, and a defoaming agent. The other two oils were the same lubricant referred to above, but to each an S-P additive package and an ATF additive package were respectively added. Through these tests, a study was made of their surface failure, rolling fatigue strength, and other prorerties.
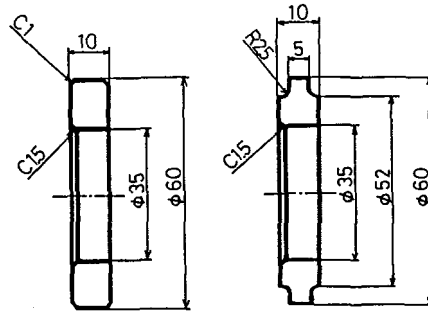
2. TEST ROLLERS

Rollers employed in this experiment were manufactured from chromium steel SCr420H, and its chemical composition is shown in Table 1. The shapes and dimensions of test rollers are shown in Figure 1. The round bar material was machined to the shape and size of the faster roller shown in Fig.1. The roller was then carburized and hardened in a heat treatment system shown in Figure 2. The faster roller was finished by grinding it to a width of 10mm and an outside diameter of 60mm. The slower roller was fabricated by grinding the 10mm wide faster roller further to a width of 5mm. The slower roller, therefore, had the carburized/hardened layer removed from its sides. These test rollers had a surface roughness of approximately 3.0μm Rmax determined axially.

Figure 3 shows the hardness and residual stress distributions of the test rollers. The same methods as those previously reported[1] were used to determine residual stress and to correct this residual stress. The roller's axial and circumferential residual stresses

Table 1 Chemical compositions (wt.%) of material

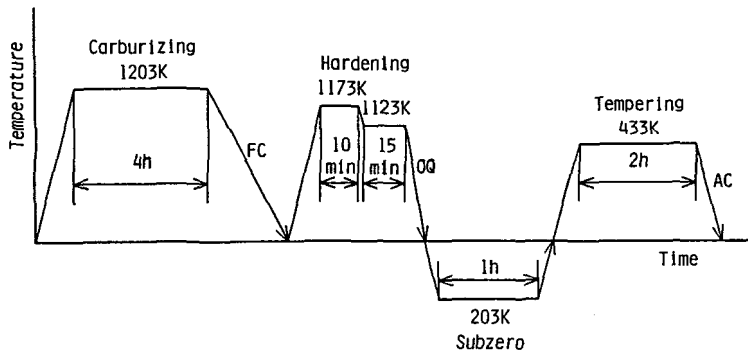| Material	C	Si	Mn	P	S	Cu	Ni	Cr
SCr420H	0.21	0.22	0.80	0.020	0.016	0.09	0.06	1.15

Fig.1 Shapes and dimensions of test rollers
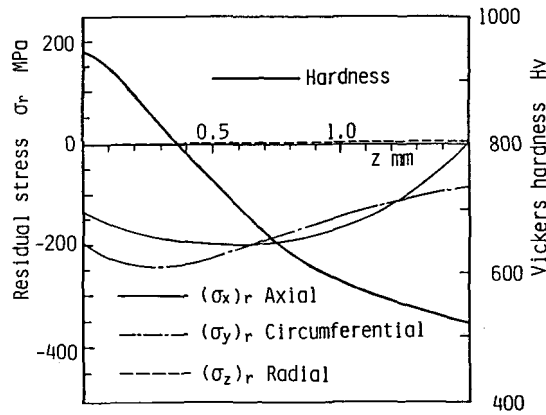
Fig.2 Heat treatments of test rollers

Fig.3 Hardness and residual stress
distributions of slower roller

$(\sigma_x)r$ and $(\sigma_y)r$ showed similar distribution trends. These stresses had compression up to approximately 1.5mm in the subsurface of the rollers. Surface hardness was Hv942 and the effective hardened depth was 1.25mm.

3. EXPERIMENTAL PROCEDURES

     The test equipment employed was a spring-loaded, rolling fatigue tester[1]. Using a combination of identical materials, the experiment was conducted under the sliding/rolling contact conditions. The faster roller was set to a rotating speed of 1800rpm and to a circumferential velocity of 5.65m/s. The slower roller was set to 1432rpm and to 4.50m/s, respectively. The specific slidings was +20.4% for the faster roller and -25.7% for the slower roller. The test equipment was provided with a vibration sensor switch. Once the roller failed on the surface, vibrations would cause the test equipment to stop automatically. The number of this automatic stop was reckoned as the fatigue life.

     Table 2 shows the physical and chemical properties of the oils tested. Oil A was a mineral base oil containing a viscosity index improver, an anti-oxidant, and a defoaming agent. Oil B was Oil A to which an S-P additive package had been added. And Oil C was Oil A with an ATF additive package added. These oils did not display significant differences in specific gravity, flash point, pour point, viscosity, and viscosity index. These lubricants were applied under pressure at a rate of approximately 2.0 liters per minute on the

Table 2 Characteristics of test oils

Oil		A (Base oil)	B (S-P additive)	C (ATF additive)
Specific gravity 288/277K		0.8875	0.8933	0.8923
Flash point K		467	455	463
Pour point K		240.5	240.5	243.0
Viscosity	313K	91.89×10^{-6}	99.83×10^{-6}	119.3×10^{-6}
m^2/s	373K	16.52×10^{-6}	17.45×10^{-6}	19.58×10^{-6}
Viscosity index		195	192	187
Total acid number mgKOH/g		0.08	0.85	0.25
Additive component	Sulphur wt.%	0.10	1.10	0.29
	Phosphorus p.pm	———	570	170
	Boron p.pm	———	40	190

engaging side of the rollers, with their temperatures controlled to
353±4K.

4. EXPERIMENTAL RESULTS AND DISCUSSION

4.1 Roller Surface Temperature and Frictional Coefficient

Figure 4 shows the results of determining the slower roller
surface temperature and inter-roller frictional coefficient. To
determine the roller surface temperature, a thermocouple was mounted
in contact with the roller surface at a delay of 90 degrees from the
roller contact position. The inter-roller frictional coefficient was
obtained by correcting the bearing loss torque, with the roller drive
torque determined by means of a resistance wire strain meter. In the
case of Oil C, roller surface temperature was found slightly higher,
while the frictional coefficient was also a little larger. Within the
range of the experiment (Hertz stress p_{max}=1750 through 2100MPa·),
however, the temperature difference among the lubricants tested was a
maximum 13K, with a maximum frictional coefficient difference of
0.003. It can be said that neither roller surface temperature nor
frictional coefficient differed significantly for each type of oil.
Figure 5 shows the relationship between roller surface temperature T
and µPVs, based on the results of Fig.4. In Fig.5, µ represents the

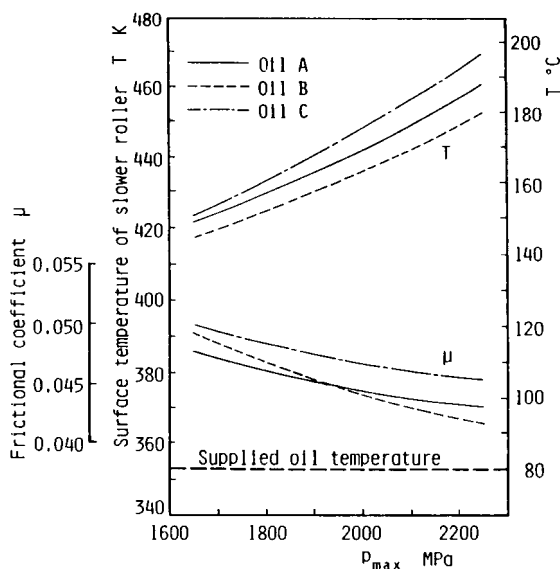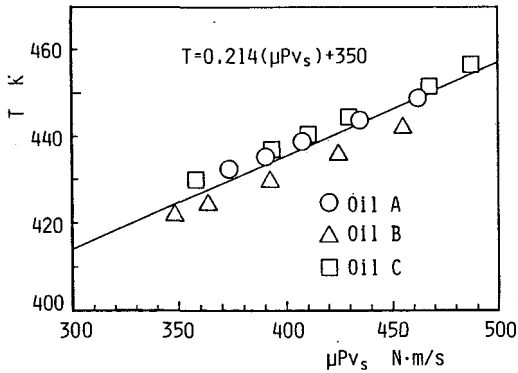Fig.4 Surface temperature of slower roller
and frictional coefficient

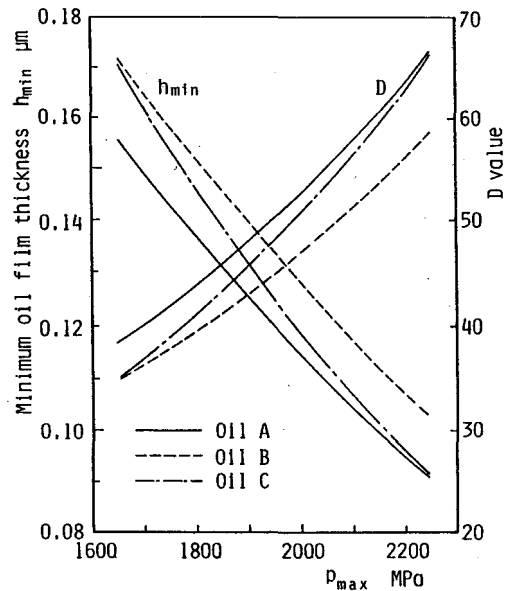Fig.5 Relationship between roller
surface temperature and μPVs

Fig.6 Theoretical minimum oil film
thickness and D-value

frictional coefficient, P the normal load (N) and Vs the sliding velocity (meters per second). Both were found to have a linear relationship of $T=0.214(\mu PVs)+350$.

Figure 6 shows changes in theoretical minimum oil film thickness hmin[2] and D-value[3], coupled with a change in Hertz stresses, as obtained on the assumption that inter-roller oil temperature was equal to the slower roller surface temperature shown in Fig.4. The D-value was found slightly lower in Oil B which showed a somewhat lower level of both roller surface temperature and frictional coefficient. As shown in Table 2, however, roller surface temperature did not vary among oil types so significantly. As a result, no significant difference was found in either hmin or D-value caused by oil type. In this experiment, the D-value exhibited a high level generally. Asperities on the roller surface might be considered to have caused metal contact.

4.2 Surface Damage

An example of surface failure caused by the rolling fatigue test is shown in Figure 7 using Oil A. In this experiment, the spalling failure shown in Fig.7 took place on every roller irrespective of oil type. As shown in Fig.7(a), spalling took place over the full width of a 5mm wide slower roller. As clearly seen from the failed roller's
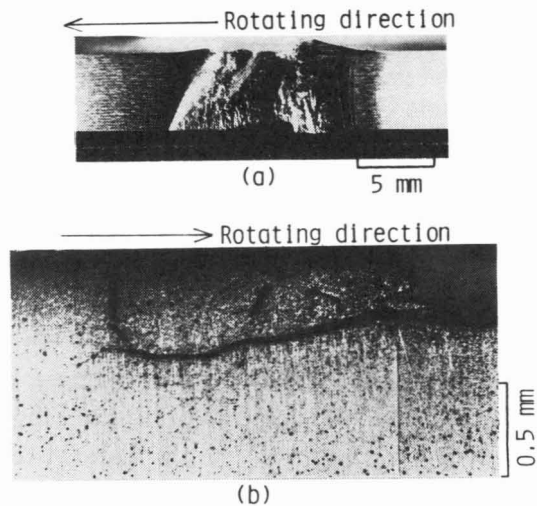
Oil A P_{max}=2100MPa   N=1.0x10^6
Fig.7 Observation of failed roller

Table 3   Rolling contact fatigue life and failure depth

Oil A			Oil B			Oil C		
P_{max} MPa	N	Failure depth μm	P_{max} MPa	N	Failure depth μm	P_{max} MPa	N	Failure depth μm
		Min-Max			Min-Max			Min-Max
1850	1.8x10^7	310-710	1750	2.1x10^7	275-550	1750	3.6x10^7	275- 405
1900	8.0x10^6	220-770	1800	1.5x10^7	300-700	1800	1.1x10^7	330- 520
1950	8.3x10^6	335-765	1900	6.4x10^6	320-575	1850	1.0x10^7	270- 625
2025	2.1x10^6	460-870	2000	1.2x10^6	400-790	1900	6.5x10^6	300- 690
2100	1.0x10^6	460-880	2100	4.3x10^5	500-850	1950	3.7x10^6	370- 800
						2050	2.1x10^6	470- 820
						2100	1.1x10^6	435-1400

axial rectangular section photo in Fig.7(a), spalling cracks occurred
on the roller subsurface nearly parallel with the roller surface.
Table 3 shows the results of determining the life and spall depth as a
result of the rolling fatigue test. The spall depth was determined by
the use of dial gage to which a stylus with a tip radius of 0.1mm was
attached. Table 3 shows the minimum and maximum spall depths. These
depths showed a tendency to increase as Hertz stress p_{max} got larger.
No definitive tendency, however, could be observed and attributed to
the difference of oil. The spalling cracks shown in Fig.7(b) had a
depth of approximately 430μm under the roller surface. Compared with
the results shown in Table 3, it can be said that the depth of the

spalling cracks was near the minimum spall depth.

4.3 Rolling Fatigue Strength

Figure 8 shows the relationsip between Hertz stress p_{max} as a result of the rolling fatigue test and life N, that is, a p_{max}-N curve. As in the results for frictional coefficient and D-value, the p_{max}-N curve did not generally vary significantly among oil types. In Fig.8, Oil B showed a slightly shorter life. Judging from the frictional coefficient and D-value, Oil B might be considered to have a relatively long life when pitting resulted from cracks occurring on the surface. In this experiment, however, spalling arose from cracks occurring on the subsurface under every condition involved. As a result, the life might be considered hardly affected by either frictional coefficient or D-value. According to the results of bench-testing helical gears manufactured from carburized and hardened steel with a lubricant less viscous than that employed in this experiment, a lubricant equivalent to Oil C with an ATF additive package added had a relatively long life of pitting. That case, however, was an accelerated life test subject to severer operating conditions. Under the conditions of this experiment or normal working conditions, the test lubricants might scarcely influence the surface durability of carburized/hardened helical gears.

In a low Hertz stress range of p_{max}=1750 through 1850MPa and in a high Hertz stress range of p_{max}=2100MPa, rollers already subjected to a rolling fatigue test were analyzed for each oil type using a X-ray microanalyzer. Results showed a large amount of oxygen found entirely on the surface of every roller. Under higher stress conditions, oxygen existed in larger amounts than under low stress conditions, hardly varying for all oil types. As with oxygen, phosphorus was detected on
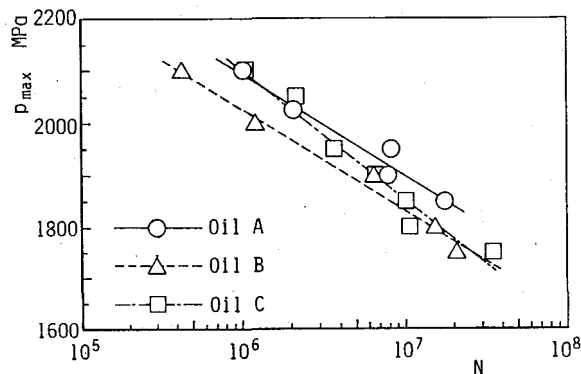

Fig.8 p_{max}-N curves

every surface. But compared with oxygen, it existed in small amounts. For Oil B, no difference in phosphorus could be found between high and low stresses conditions. However, a larger amount of phosphorus was present with Oil B than with Oil C. Sulfur was scarecely detected under high stress conditions but was slightly segregated under low stress conditions. A larger amount of sulfur was detected with Oil B than with Oil C. Boron was not detected in any of the oils tested. From these results of analysis using a X-ray microanalyzer and of Fig.8, it was found that if an extreme pressure film formed containing sulfur and phosphorus, especially sulfur, would decrease the fatigue life somewhat.

4.4 Discussion

The spalling which took place in these experiments might have a relationship with the shear stresses whose values become maximum beneath the surfaces of contact rollers. To examine the experimental results on spalling failure and rolling fatigue strength, the maximum value $[A(\tau/Hv)]$max of amplitude $A(\tau/Hv)$ for the ratio of shear stress to roller subsurface hardness Hv and the depth beneath the contact surface at which the amplitude maximized, were obtained on the assumption that material strength was proportional to the hardness and that the effects of mean stresses upon fatigue were negligible as previously reported[4]. The shear stresses taken into consideration here were orthogonal shear stress τ_{yz} and maximum shear stress $\tau_{45°}$. To calculate the shear stresses, the analytical results obtained by J.O.Smith[5] were used. To calculate τ/Hv, consideration was given to initial residual stress distribution and initial hardness distribution in the test rollers shown in Fig.3, and the actual inter-roller frictional coefficoent determined under each of the operating conditions shown Fig.4. Figure 9 shows the coordinates for calculating subsurface stress of contacting rollers. Figure 10 shows an example of $\tau_{45°}/Hv$ and τ_{yz}/Hv distributed on plane yz calculated as described above, with Oil A applied at p_{max}=1900MPa. With attention to fixed point on the subsurface, it cuold be formed from Fig.10 that τ_{yz}/Hv oscillated bilaterally and $\tau_{45°}/Hv$ exhibited a unidirectional oscillating change, coupled with the movement of a roller contact position.

Table 4 shows examples of each oil's calculation results for Oil A in relation to maximum value $[A(\tau_{yz}/Hv)]$max of the amplitude for a ratio of bilaterally oscillating orthogonal shear stress to hardness,
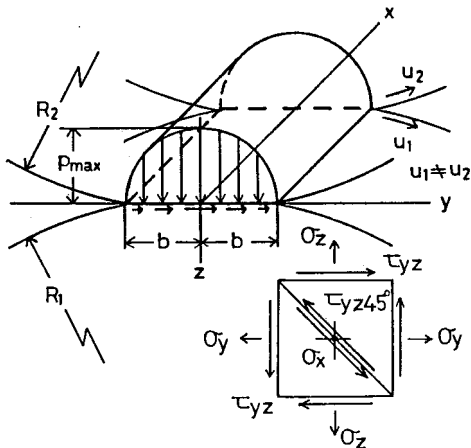
Fig.9 Coordinates and stress
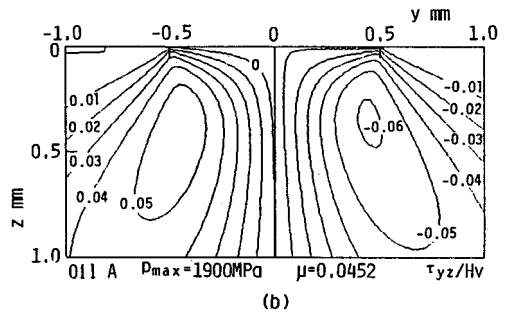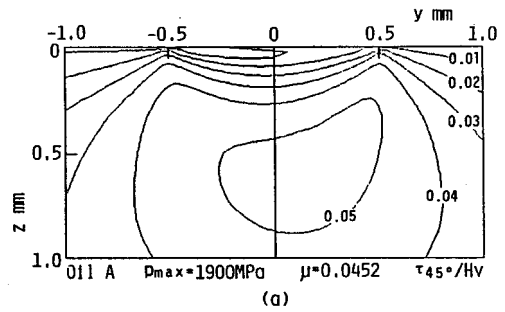   components in contacting
      rollers

Fig.10 τ/Hv distributions
       on yz plane

Table 4   Values of maximum amplitudes $[A(\tau_{yz}/Hv)]$max and
          $[A(\tau_{45°}/Hv)]$max, and these occurring depths Z

Oil A

P_{max} MPa	μ	T K	$A(\tau_{yz}/Hv)$			$A(\tau_{45°}/Hv)$		
			A_{max}	z mm	Hv	A_{max}	z mm	Hv
1700	0.0472	423.9	0.0514	0.325	813	0.0195	0.225	861
1800	0.0462	429.5	0.0550	0.325	813	0.0212	0.400	780
1900	0.0452	435.6	0.0586	0.350	802	0.0237	0.650	677
2000	0.0445	442.1	0.0624	0.400	780	0.0266	0.700	659
2100	0.0438	449.0	0.0663	0.425	769	0.0296	0.750	642
2200	0.0433	456.7	0.0701	0.450	758	0.0326	0.750	642

ν= 0.3   E= 206 GPa

maximum value $[A(\tau_{45°}/Hv)]$max of the amplitude for a ratio of
unidirectionally oscillating maximum shear stress to hardness, these
occurrence depth Z, and the hardness at these depths. As shown in
Fig.4, the inter-roller frictional coefficient hardly varied among oil
types. The results shown in Table 4 were found nearly identical with
those for Oils B and C. From Table 4, it may be considered that
maximum amplitude value Amax and its occurrence depth Z increase with
an increase in Hertz stress, and this concides quantitatively with the
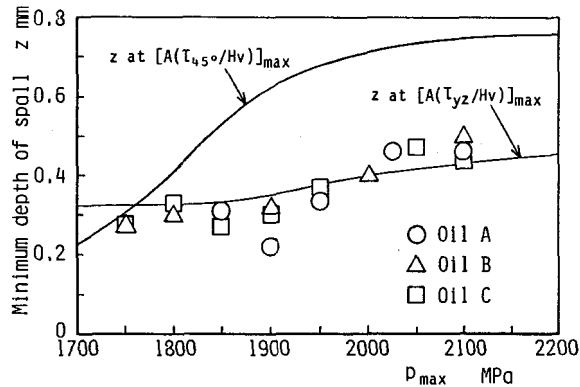results in Table 3. Figure 11 shows the relationship between the

Fig.11 Relationship between spall depth and
depth at maximum amplitude Amax

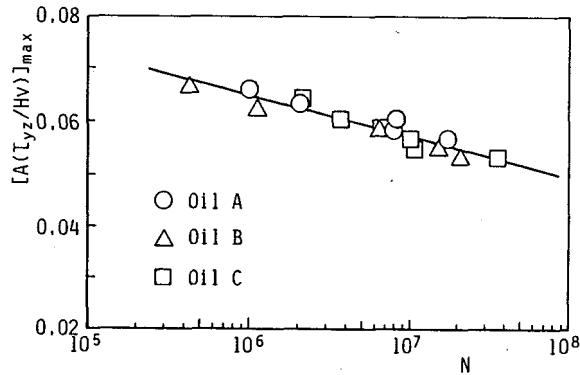Fig.12 $[A(\tau_{yz}/Hv)]$max-N curve

depth at which $[A(\tau_{yz}/Hv)]$max and $[A(\tau_{45°}/Hv)]$max were attainable
under each Hertz stress condition and the minimum spall depth for all
of the test oils. The spalling crack depth can be considered near the
minimum spall depth. From Fig.11, therefore, it can be considered
that spalling cracks occurred over a depth range of $[A(\tau_{45°}/Hv)]$max
through $[A(\tau_{yz}/Hv)]$max. This tendency held true even when the oil was
changed. And it also coincided well with results previously
reported[6]. Thus, spalling cracks occur depending upon
$[A(\tau_{yz}/Hv)]$max. Figure 12 shows the relationship between maximum
amplitude value $[A(\tau_{yz}/Hv)]$max and life N, i.e. Amax-N curve, from the
results shown in Table 3 and 4. Each of the plot points were
expressed as a single Amax-N curve, irrespective of the different
types of oil. As such, the type of oil was seem to seldom affect the
Amax-N curve.

5. CONCLUSION

To clarify the effects of a drive system lubricant additive upon the rolling fatigue of carburized and hardened steel rollers, a sliding/rolling fatigue test was conducted using three types of oil as lubricants: a mineral base oil containing a viscosity index improver, an antioxidant, and a defoaming agent, and two mineral base oils to which S-P and ATF additive packages were added, respectively. And a study was made concerning the failure to the surface, rolling fatigue strength, and then factors. The results are summarized as follows:

(1) Roller surface temperature, inter-roller frictional coefficient, theoretical minimum oil film thickness, and D-value were hardly affected by the type of oil within the range of this experiment.

(2) Every failure taking place on the surface in this experiment was spalling caused by roller subsurface cracks, irrespective of oil type. Also, spalling failure depth did not vary among oil types. And spalling depth tended to increase as Hertz stresses got larger. Spalling crack occurrence depth in all oil types nearly coincided with that at which amplitude $A(\tau_{yz}/Hv)$ for the ratio of bilaterally oscillating orthogonal shear stress to hardness reached the maximum.

(3) Rolling fatigue strength did not vary significantly for all types of oil. Within the range of this experiment, however, it can be said that the formation of an extreme pressure coated film containing sulfur and phosphorus would have a minor negative effect on fatigue life. The curve showing the relationship between maximum amplitude value $[A(\tau_{yz}/Hv)]max$ and life N, i.e. $[A(\tau_{yz}/Hv)]max$-N curve, could be expressed as a single curve for all of the oils tested.

REFERENCES

 (1) K.FUJITA and A.YOSHIDA: Wear,43,3(1977),301.
 (2) D.DOWSON: Proc.Instn.Mech.Engrs.,182,3A(1967-68),151.
 (3) P.H.DAWSON: Proc.Instn.Mech.Engrs.,180,3B(1965-66),95.
 (4) K.FUJITA and A.YOSHIDA: Bull.JSME,23,178(1980),587.
 (5) J.O.SMITH and C.K.LIU: J.Appl.Mech., Trans.ASME,20(1953),157.
 (6) A.YOSHIDA, K.FUJITA and K.MATSUO: J.JSLE, Int.Ed.,7(1986),71.